ELECTRONIC SUPPLEMENTARY INFORMATION (ESI)

$V^{IV}O$ and Cu^{II} complexation by ligands based on pyridine nitrogen donors

Daniele Sanna,[a] Péter Buglyó,[b] Ana Isabel Tomaz,[c] Joao Costa Pessoa,*[d] Slađana Borović,[d] Giovanni Micera[e] and Eugenio Garribba*[e]

[a] *Istituto CNR di Chimica Biomolecolare, Trav. La Crucca 3, I-07040 Sassari, Italy*

[b] *Department of Inorganic and Analytical Chemistry, University of Debrecen, H-4010 Debrecen, Hungary*

[c] *Centro de Ciências Moleculares e Materiais, Departamento de Química e Bioquímica, Universidade de Lisboa, Campo Grande, 1749-016 Lisboa, Portugal*

[d] *Centro de Química Estrutural Instituto Superior Técnico, Universidade Técnica de Lisboa, Av. Rovisco Pais, 1049-001 Lisboa, Portugal. E-mail: joao.pessoa@ist.utl.pt; Fax: +351 218419239; Tel: +351 218419268*

[e] *Dipartimento di Chimica e Farmacia, and Centro Interdisciplinare per lo Sviluppo della Ricerca Biotecnologica e per lo Studio della Biodiversità della Sardegna, Università di Sassari, Via Vienna 2, I-07100 Sassari, Italy. E-mail: garribba@uniss.it; Fax: +39 079 229559; Tel: +39 079 229487*

Table S1 Structural parameters calculated from the DFT simulations on the $V^{IV}O$ complexes and comparison with similar species reported in the literature.[a]

Complex [b]	V=O	V–N^{eq}	V–N^{ax}	V–O	O=V–N^{eq}	O=V–N^{ax}	O=V–O	θ [c]	Ref.
$[VO(phen)(H_2O)_3]^{2+}$ (eq-eq)	1.576	2.084, 2.087	–	2.110, 2.113, 2.216	101.18, 102.06	–	89.2, 90.0, 165.8	95.4, 96.5	*d*
$[VOCl_2(phen)(CH_3OH)]$	1.627	2.149, 2.152	–	–	95.0, 95.6	–	–	91.5, 94.1	46
$[VO(phen)(H_2O)_3]^{2+}$ (eq-ax)	1.587	2.092	2.244	2.065, 2.071, 2.071	91.79	167.83	94.1, 94.1, 102.7	180.0	*d*
$[VOF_2(phen)(H_2O)]$	1.624	2.133	2.306	2.013	92.72	166.27	104.1	172.0	45
cis-$[VO(phen)_2(H_2O)]^{2+}$	1.589	2.098, 2.106, 2.114	2.279	2.108	100.9, 102.1, 92.9	164.7	89.6	96.6, 94.9, 171.6	*d*
cis-$[VO(phen)_2(SO_4)]$	1.585	2.121, 2.136,	2.324	1.959	95.1, 103.5, 96.3	169.6	103.4	94.1, 104.2, 174.9	51
cis-$[VO(phen)_2(OH)]^{+}$	1.605	2.117, 2.210, 2.124	2.336	1.848	102.4, 90.1, 91.2	160.0	109.4	96.3, 80.6, 173.3	*d*
cis-$[VO(phen)_2(OH)]^{+}$	1.678	2.113, 2.173, 2.112	2.247	1.778	97.4, 90.3, 92.7	163.8	106.3	90.5, 80.7, 173.7	52
$[VO(bpy)(H_2O)_3]^{2+}$ (eq-eq)	1.577	2.072, 2.075	–	2.116, 2.117, 2.216	101.2, 102.2	–	88.8, 88.9, 165.2	94.8, 96.0	*d*
[VO(bpy)(METIDA)]	1.602	2.088, 2.094	–	1.969, 1.982	99.2, 99.5	–	100.6, 102.9	98.0, 95.1	57
$[VO(bpy)(H_2O)_3]^{2+}$ (eq-ax)	1.588	2.090	2.220	2.073, 2.073, 2.067	91.9	166.8	93.9, 93.9, 102.6	179.9	*d*
$[VO(Me_2bpy)(PhS)_3]^{-}$	1.611	2.156	2.331	–	92.2	163.0	–	178.5	58
cis-$[VO(bpy)_2(H_2O)]^{2+}$	1.590	2.087, 2.095, 2.115	2.256	2.113	101.3, 101.9, 92.7	163.5	89.3	94.9, 96.8, 170.6	*d*
cis-$[VO(bpy)_2(SO_4)]$	1.585	2.101, 2.142, 2.117	2.296	1.957	95.3, 101.9, 94.2	166.5	105.0	97.0, 105.0, 174.0	56
cis-$[VO(bpy)_2(OH)]^{+}$	1.609	2.117, 2.186, 2.131	2.300	1.851	90.3, 101.9, 90.4	158.6	109.4	79.2, 94.1, 173.2	*d*
cis-$[VO(bpy)_2(OH)]^{+}$	1.687	2.114, 2.175, 2.113	2.247	1.761	89.5, 100.1, 93.1	161.7	106.2	83.5, 98.7, 178.5	56
$[VO(terpy)(H_2O)]^{2+}$	1.588	2.091, 2.022, 2.091	–	2.078	102.9, 112.7, 02.97	–	100.6	99.8, 88.8, 99.8	*d*
$[VO(terpy)(SO_4)]$	1.594	2.124, 2.037, 2.132	–	1.996, 2.239	97.0, 107.6, 96.3		102.4, 169.2	103.3, 93.8, 103.9	59
$[VO(terpy)(H_2O)_2]^{2+}$	1.597	2.102, 2.102	2.152	2.082, 2.082	105.4, 105.5	180.0	90.9, 90.9	180.0, 180.0	*d*
$[VO(terpy)(HPO_3(Ph))_2]$	1.601	2.129, 2.137	2.176	2.001, 2.001	104.3, 108.6	177.1	99.4, 96.1	172.8, 176.0	60
$[VO(terpy)(OH)]^{+}$	1.588	2.116, 2.070, 2.116	–	1.814	100.4, 112.3, 101.7	–	116.9	103.1, 88.2, 101.2	*d*

$[VO(terpy)(OH)(H_2O)]^+$	1.619	2.113, 2.120	2.160	2.210, 1.819	103.4, 105.9	158.0	79.7, 110.5	157.8, 159.9	*d*

[a] Bond distances reported in Å, and angles in °. [b] METIDA is *N*-methoxyiminodiacetate, Me_2bpy is 4,4'-dimethyl-2,2'-bipyridine and HPO_3(Ph) is hydrogen phenylphosphonato. [c] Mean value of the two dihedral angles between V=O and the two N–C aromatic bonds of the equatorially coordinated pyridine rings. [d] Structure simulated in this work by DFT calculations.

Table S2 Experimental and calculated spin Hamiltonian parameters of the $V^{IV}O$ complexes measured in frozen (120 K) aqueous solution.

Complex	V–V [a]	V–O–V [b]	g^{exptl}	A^{exptl} [c]	D^{exptl} [d]	J^{calcd} [d,e]
$[(VO)_2(phen)_2(H_2O)_2(OH)_2]^{2+}$	3.309	107.7	1.979	81.3	0.0626	5.24
$[(VO)_2(bpy)_2(H_2O)_2(OH)_2]^{2+}$	3.316	107.8	1.983	81.9	0.0641	4.91
$[(VO)_2(bpm)_2(H_2O)_2(OH)_2]^{2+}$	3.315	107.8	1.980	81.2	0.0631	4.93
$[(VO)_2(bpp)_2(H_2O)_2(OH)_2]^{2+}$	3.308	107.5	1.979	81.7	0.0634	4.74

[a] Bond distances reported in Å. [b] Angles reported in °. [c] Values reported in 10^{-4} cm^{-1}. [d] Values reported in cm^{-1}. [e] Values calculated by DFT methods.

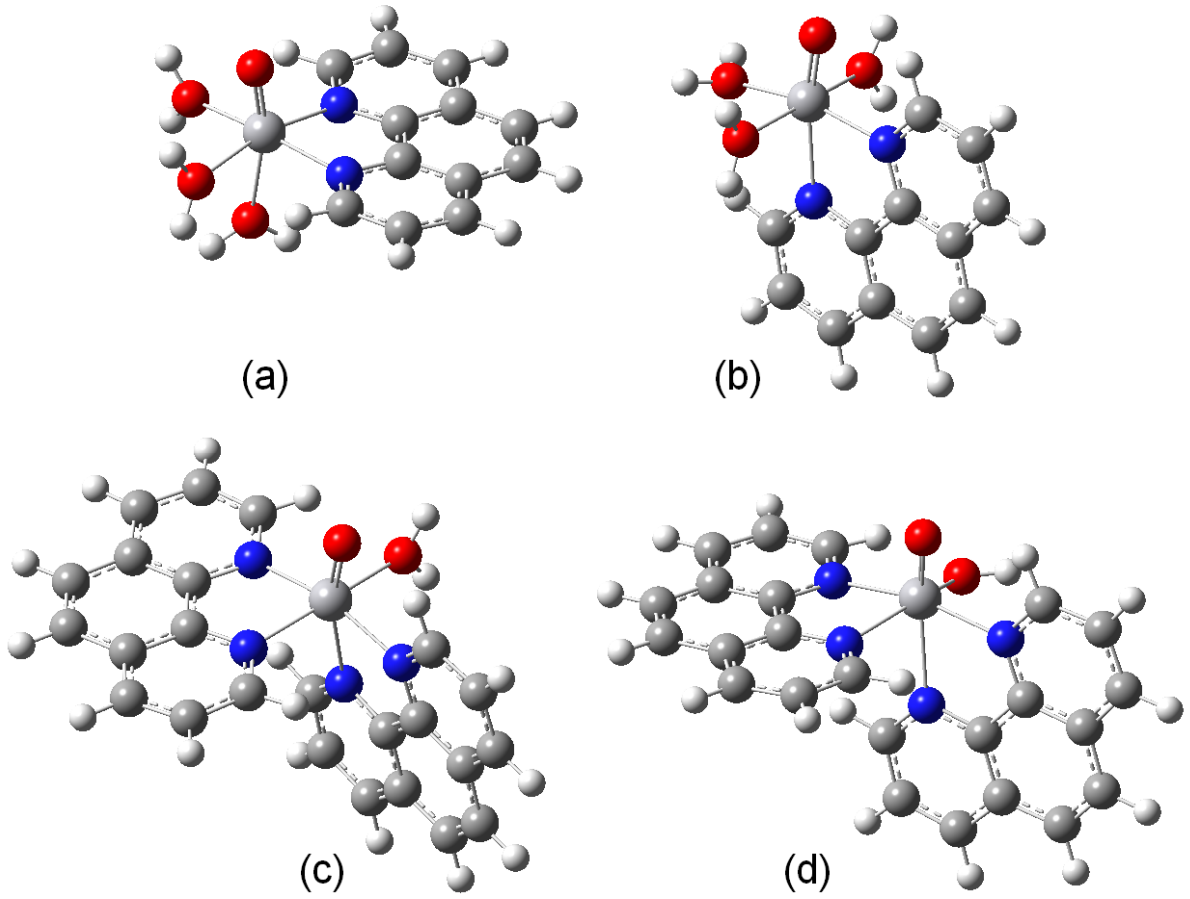

Fig. S1 Optimised structure with DFT methods at the level of theory B3P86/6-311g of the complexes formed in the system $V^{IV}O$/phen: (a) $[VO(phen)(H_2O)_3]^{2+}$ (equatorial-equatorial coordination); (b) $[VO(phen)(H_2O)_3]^{2+}$ (equatorial-axial coordination); (c) *cis*-$[VO(phen)_2(H_2O)]^{2+}$ and (d) *cis*-$[VO(phen)_2(OH)]^{+}$.

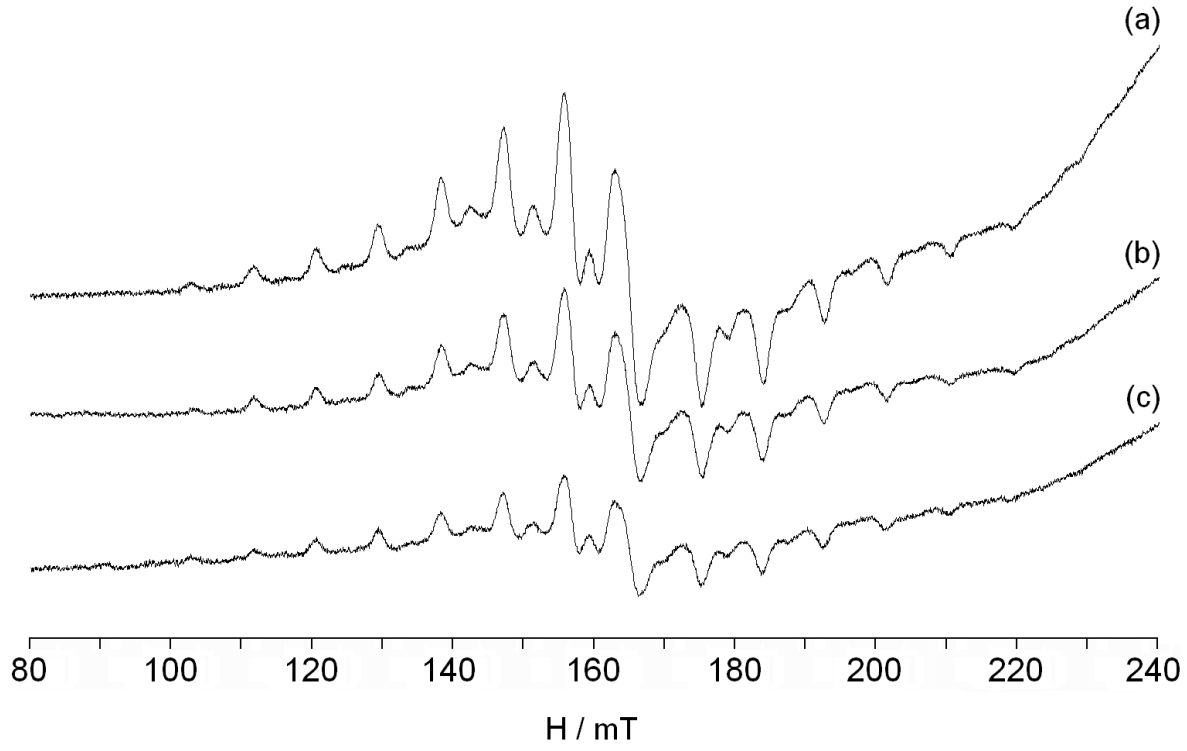

Fig. S2 Half-field region of the X-band anisotropic EPR spectra recorded at 120 K on the systems: (a) $V^{IV}O$/phen 1:1, total $V^{IV}O$ concentration of 1×10^{-2} M, pH 5.50; (b) $V^{IV}O$/bpy 1:1, total $V^{IV}O$ concentration of 5×10^{-3} M, pH 4.45 and (c) $V^{IV}O$/bpp 3:1, total $V^{IV}O$ concentration of 5×10^{-3} M, pH 4.50.

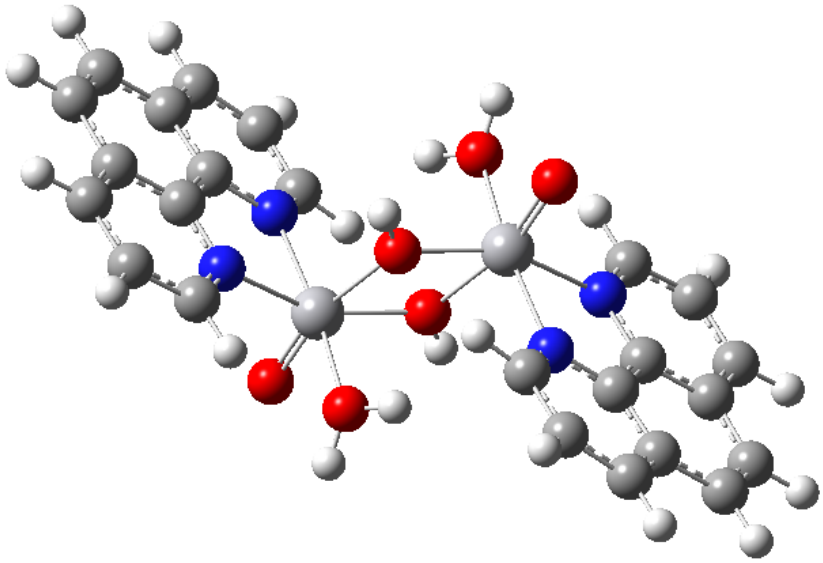

Fig. S3 Optimised structure with DFT methods at the level of theory B3P86/6-311g of the complex $[(VO)_2(phen)_2(H_2O)_2(OH)_2]^{2+}$.

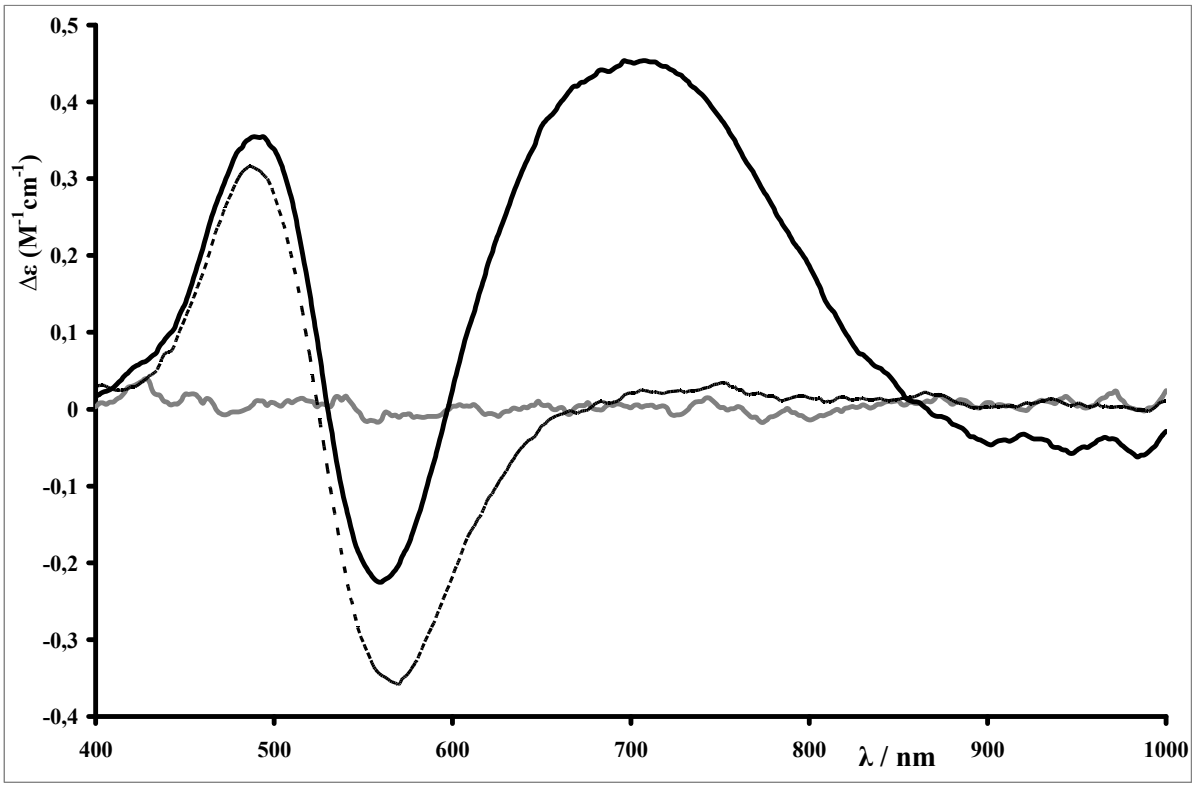

Fig. S4 CD spectra of a solution of HSA (500 μM) (grey) and upon stepwise additions of a Cu^{II} solution. (---): with a Cu:HSA molar ratio of 0.8; (——): with a Cu:HSA molar ratio of 2.0. Measurements were carried out in HEPES buffer (pH = 7.4), with a quartz cell of 2.0 cm optical path.

The Cu^{II}/HSA system produces relatively intense (for d-d bands). CD spectra in the visible region, thus reflecting its strong binding to HSA by covalent bonds, display three distinct bands in the visible range of the CD spectrum (Fig. S4 of ESI). The peaks at ~490 nm and ~560 nm have been previously associated with the binding of 1 mol equivalent of Cu^{II} at the site I, while the broad positive peak at ~700 was associated with the binding of the second mol equivalent of Cu^{II} to the site II of HSA.

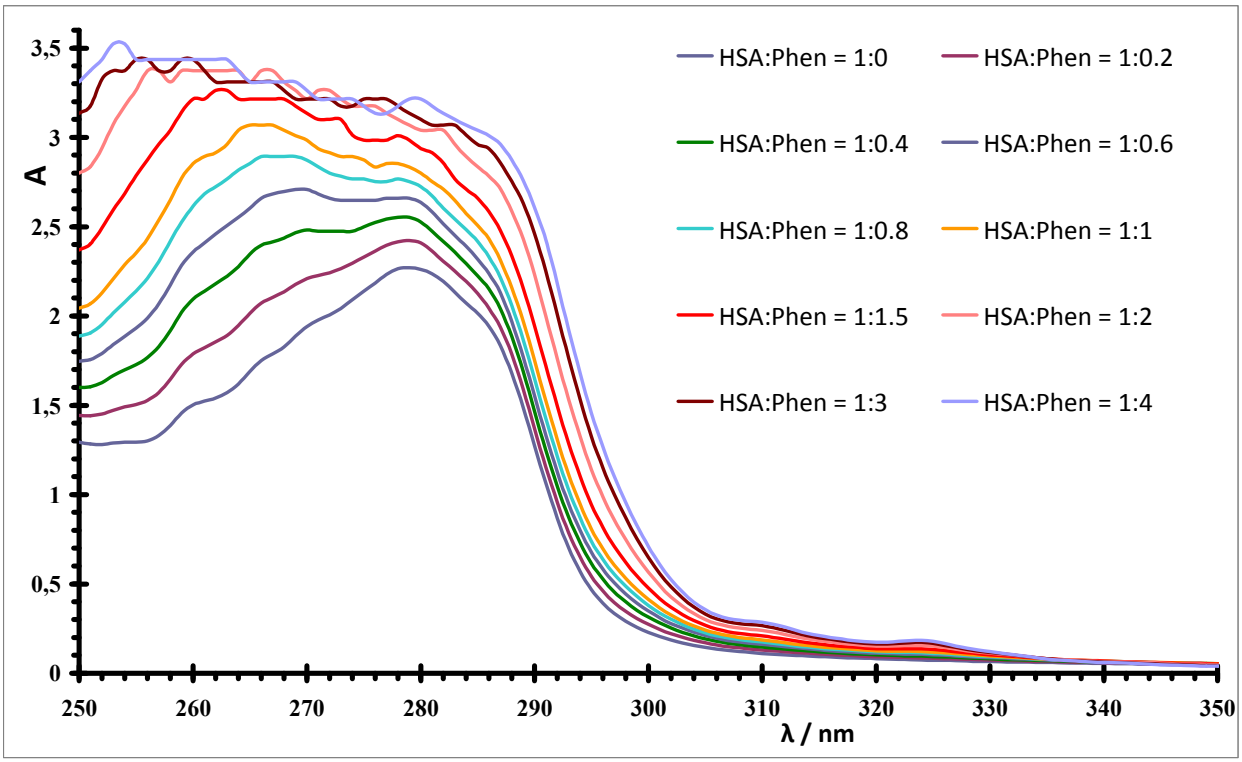

Fig. S5 UV spectra of solutions containing HSA (300 μM) upon additions of phen at pH 7.4 (PBS buffer containing 5 % of ethanol) with a 2 mm path length quartz cell.

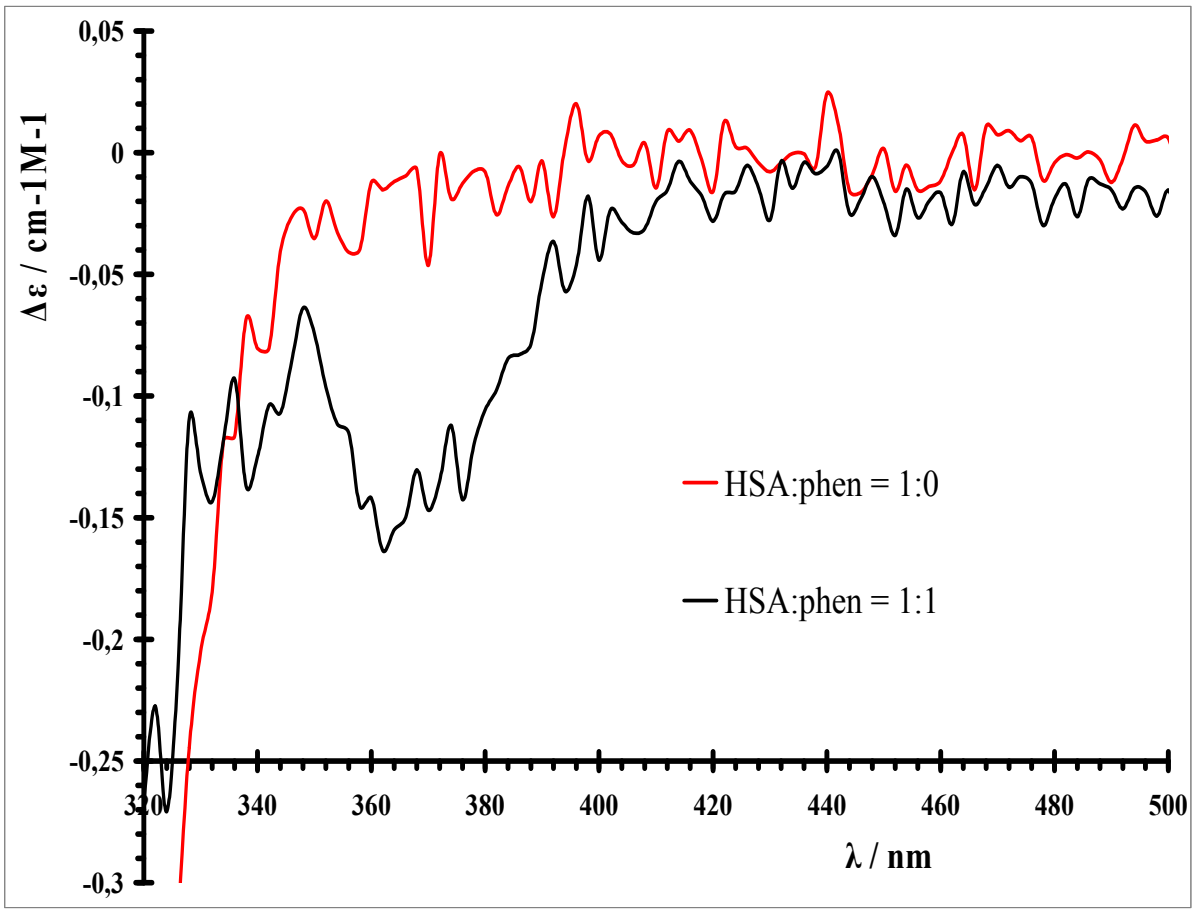

Fig. S6 Circular dichroism spectra of solutions containing HSA (250 μM) and after the addition of phen up to a HSA:phen molar ratio of 1:1. The CD spectra were recorded with a 2 cm optical path quartz cell, and in this figure are depicted without noise smoothing. The CD band recorded at ca. 360 nm is very weak. Thus the signal-to-noise ratio is not favorable and a noise reduction sub-routine (of the Jasco CD instrument software) was used to smooth the noise. For the CD spectra presented in Figs. S7 of ESI this sub-routine was used, but the noise cannot be totally smoothed, thus the spectra appear "wavy".

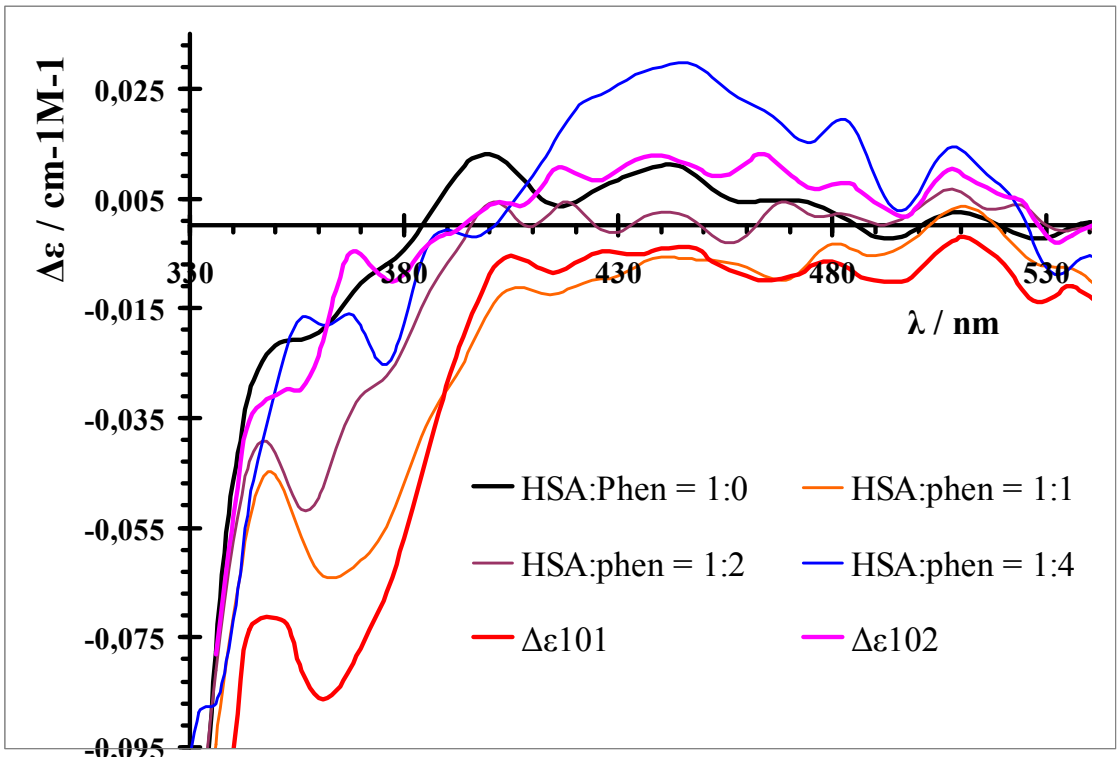

Fig. S7 Comparison of $\Delta\varepsilon_{101}$ and $\Delta\varepsilon_{102}$ values for HSA/phen system calculated by PSEQUAD with some of the experimental CD spectra measured with solutions with a total HSA concentration of ca. 300 μM. Experimental HSA:phen molar ratios are indicated; red ($\Delta\varepsilon_{101}$) represents the calculated $\Delta\varepsilon_{101}$ values and pink ($\Delta\varepsilon_{102}$) represents the calculated $\Delta\varepsilon_{102}$ values. The log values of binding constants refined were: $\log\beta_{101}$(HSA-(phen)) = 10.0 ± 0.8, and $\log\beta_{102}$(HSA-$(phen)_2$) = 14.5 ± 0.4. As the CD signals are very weak and noisy, the values of these binding constants must be taken as approximations, mainly meaning that the binding of phen to HSA is 'quantitative' at least up to a 1:1 molar ratio of HSA:phen. Note that the plot of $\Delta\varepsilon_{101}$ and $\Delta\varepsilon_{102}$ values is not a comparison of fitting of calculated vs. experimental spectra. For this one should calculate, for each λ of each experimental spectrum, the value of $\{\Delta A = \Delta\varepsilon_{101} \times C_{101} + \Delta\varepsilon_{102} \times C_{102}\}$, where C_{101} and C_{102} are the concentrations of species HSA-(phen) and HSA-$(phen)_2$ in each particular solution.

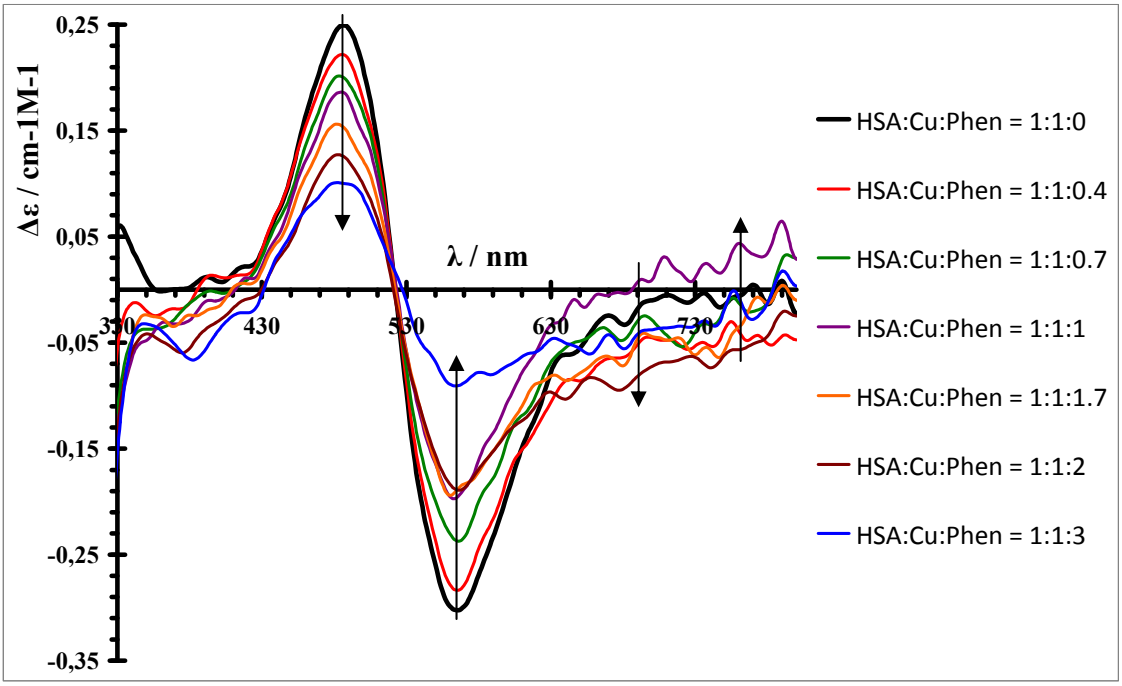

Fig. S8 CD spectra of 200 μM HSA loaded with 1.0 mol equivalent of Cu^{II} with stepwise additions of phen. The HSA:Cu:phen molar ratios are indicated. Measurements were carried out in 5% EtOH PBS buffer (pH = 7.4) with an optical path cell of 2 cm.

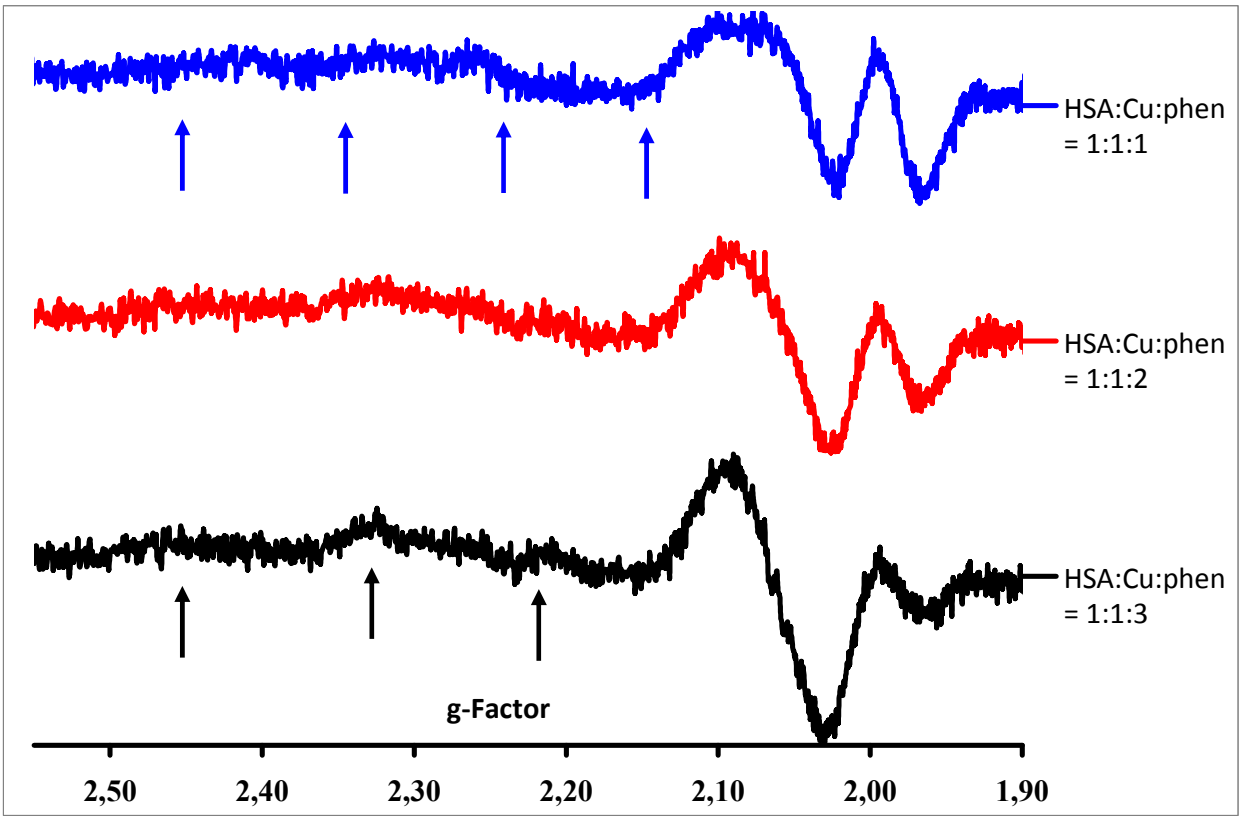

Fig. S9 X-band EPR spectra of frozen solutions (at 77 K) recorded for the system HSA/Cu^{II}/phen (solutions in 5% EtOH PBS buffer). The HSA:Cu:phen molar ratios used are indicated. The black arrows indicate where components of the EPR spectrum of solutions of Cu:phen with the molar ratio 1:3 (in 5% EtOH PBS buffer) are detected (correspond to $Cu(phen)_2$ and $Cu(phen)_3$ complexes). The blue arrows indicate where components of the EPR spectrum of solutions of HSA:Cu with the molar ratio 1:2 (in 5% EtOH PBS buffer) are detected (correspond to HSA-Cu complexes).

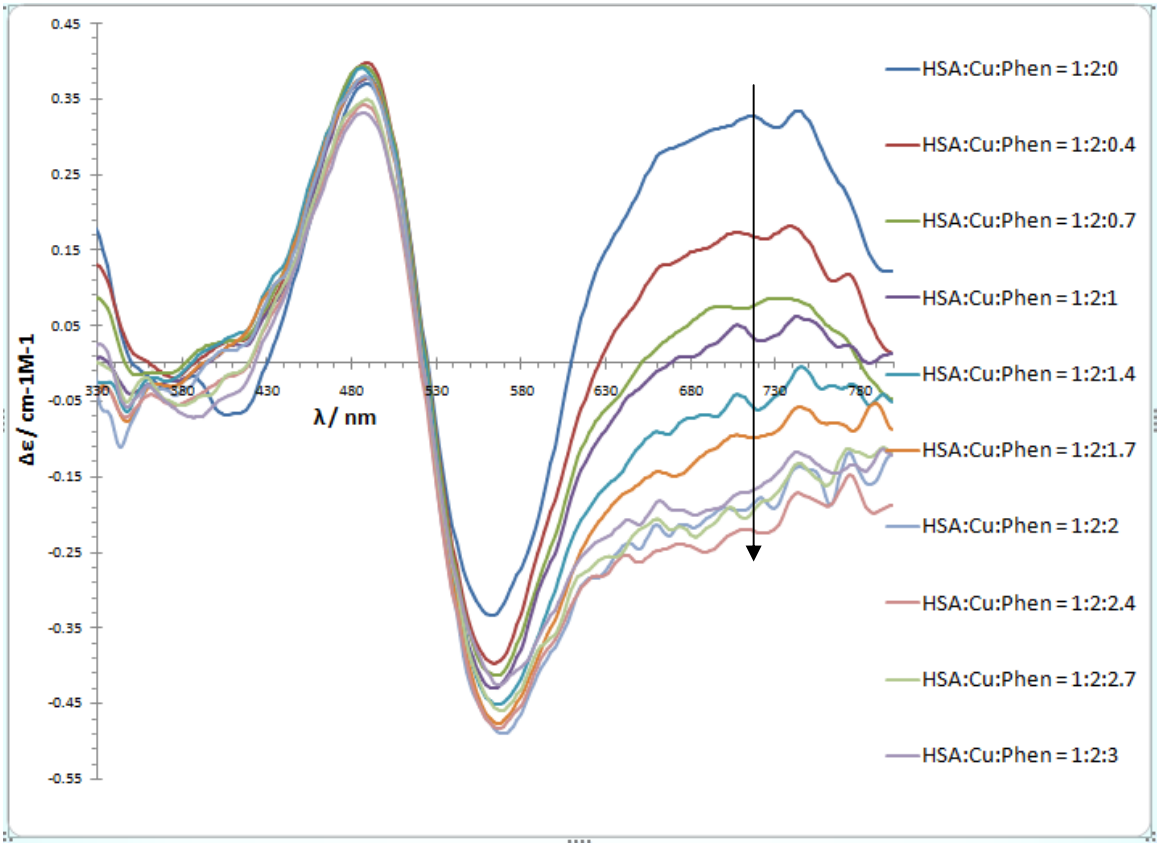

Fig. S10 CD spectra of 400 μM HSA loaded with 2.0 mol equivalents of Cu^{II} with stepwise additions of phen. The HSA:Cu:phen molar ratios are indicated. Measurements were carried out in 5% EtOH PBS buffer (pH = 7.4) with an optical path cell of 2 cm.

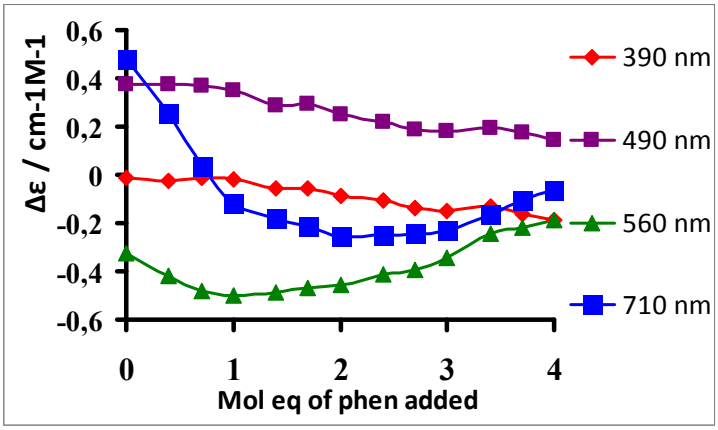

Fig. S11 Changes in spectral intensities at λ_{max} of the CD spectra depicted in Fig.7, with the additions of phen up to 4 mol eq. Measurements were carried out in 5% EtOH PBS buffer (pH = 7.4) with an optical path quartz cell of 1 cm.

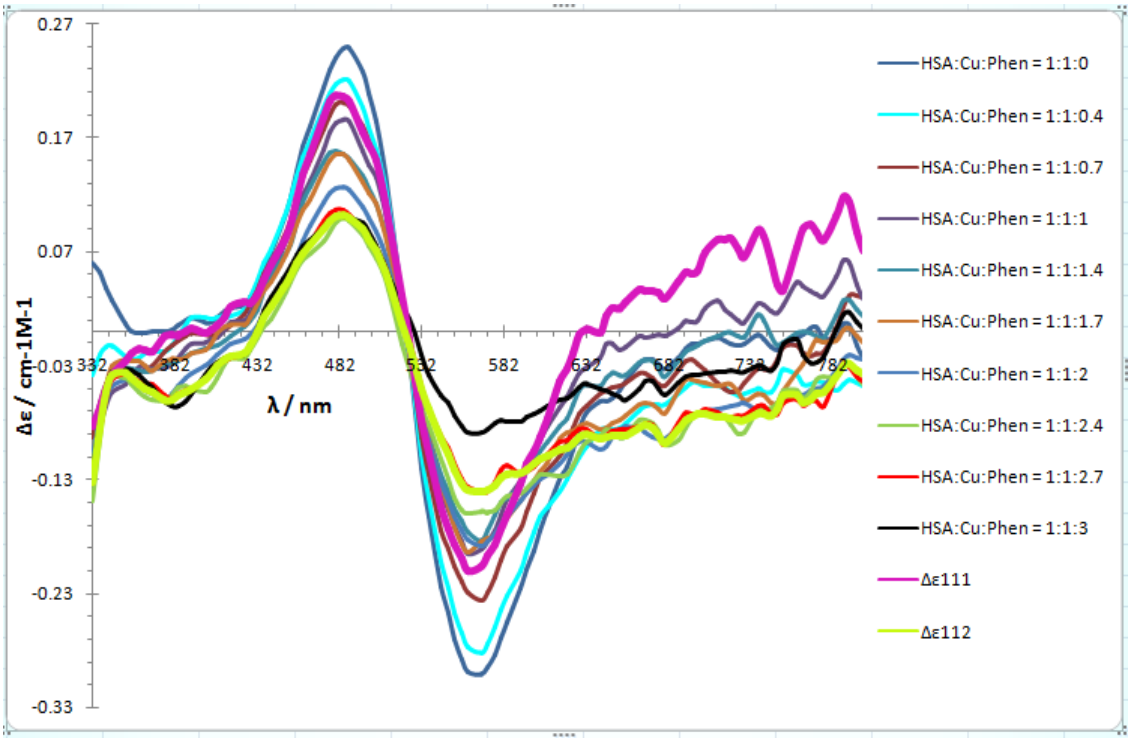

Fig. S12 Comparison of $\Delta\varepsilon_{111}$ values [of HSA-Cu-(phen)] and $\Delta\varepsilon_{112}$ [of HSA-Cu-$(phen)_2$] calculated by PSEQUAD with experimental data. The experimental HSA:Cu:phen molar ratios are indicated; pink and yellow represent the calculated $\Delta\varepsilon_{111}$ and $\Delta\varepsilon_{112}$ values, respectively. As in the case of Fig. S7 of ESI, this is not a comparison of fitting of calculated vs. experimental spectra. For this one should calculate, for each λ of each experimental spectra, the value of $\{\Delta A = \Sigma\ \Delta\varepsilon_n \times C_n\}$, where C_n are the concentrations each of the *n* species HSA-Cu_m-$(phen)_m$ contributing to the CD spectra in each particular solution.

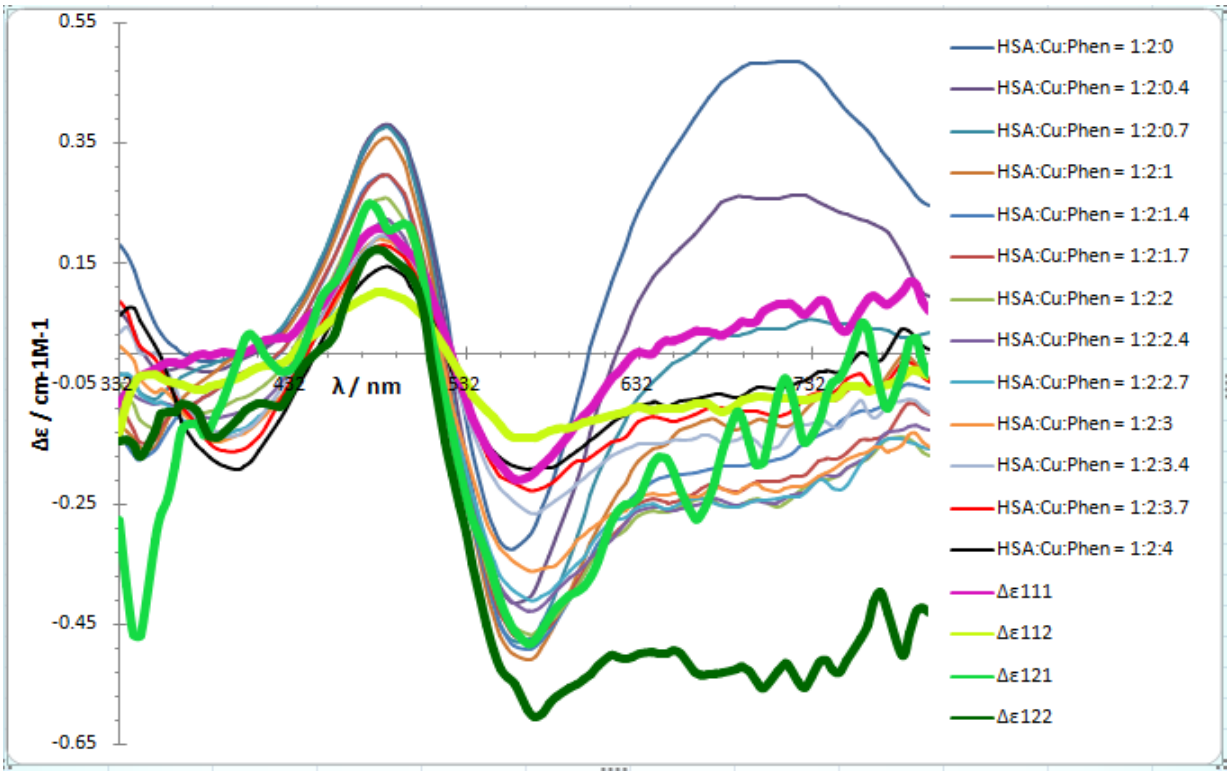

Fig. S13 Comparison of the calculated $\Delta\varepsilon_{111}$ values of HSA-Cu-(phen), $\Delta\varepsilon_{112}$ values of HSA-Cu-(phen)$_2$, $\Delta\varepsilon_{121}$ values of HSA-Cu$_2$-(phen) and $\Delta\varepsilon_{122}$ values of HSA-Cu$_2$-(phen)$_2$ obtained by PSEQUAD from the experimental data and refinement of logβ values. As in the case of previous figures, this is not a comparison of fitting of calculated vs. experimental spectra. For this one should calculate, for each λ of each experimental spectra, the value of $\{\Delta A = \Sigma\ \Delta\varepsilon_n \times C_n\}$, where C_n are the concentrations each of the *n* species HSA-Cu$_p$-(phen)$_q$ contributing to the CD spectra in each particular solution.

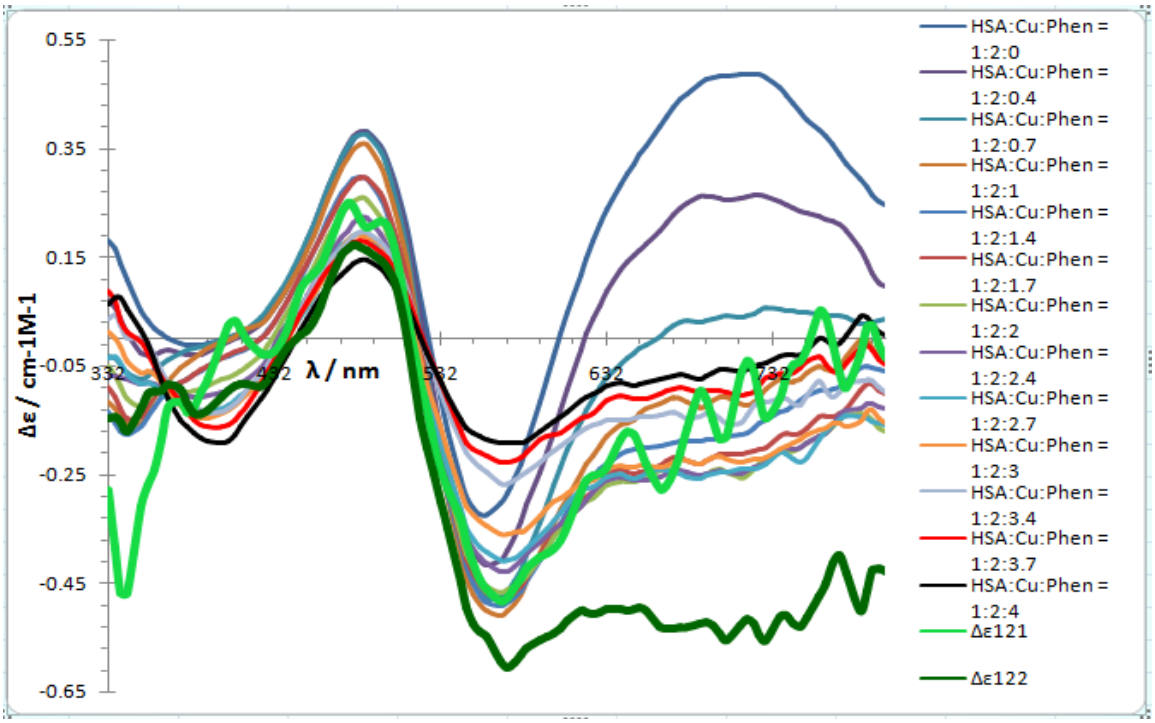

Fig. S14 Comparison of $\Delta\varepsilon_{121}$ values of HSA-Cu_2-(phen) and $\Delta\varepsilon_{122}$ of HSA-Cu_2-$(phen)_2$ calculated using the computer program PSEQUAD based on CD experimental data. The experimental HSA:Cu:phen molar ratios are indicated; light green and dark green represent the refined $\Delta\varepsilon_{121}$ and $\Delta\varepsilon_{122}$ values. The log values of the binding constants refined are: $\log\beta_{121}$ (HSA-Cu_2-(phen)) = 30.6 ± 0.1 and $\log\beta_{122}$ (HSA-Cu_2-$(phen)_2$) = 36.6 ± 0.2. As in the case of previous figures, this is not a comparison of fitting of calculated vs. experimental spectra. For this one should calculate, for each λ of each experimental spectra, the value of $\{\Delta A = \Sigma\ \Delta\varepsilon_n \times C_n\}$, where C_n are the concentrations each of the *n* species HSA-Cu_p-$(phen)_q$ contributing to the CD spectra in each particular solution.

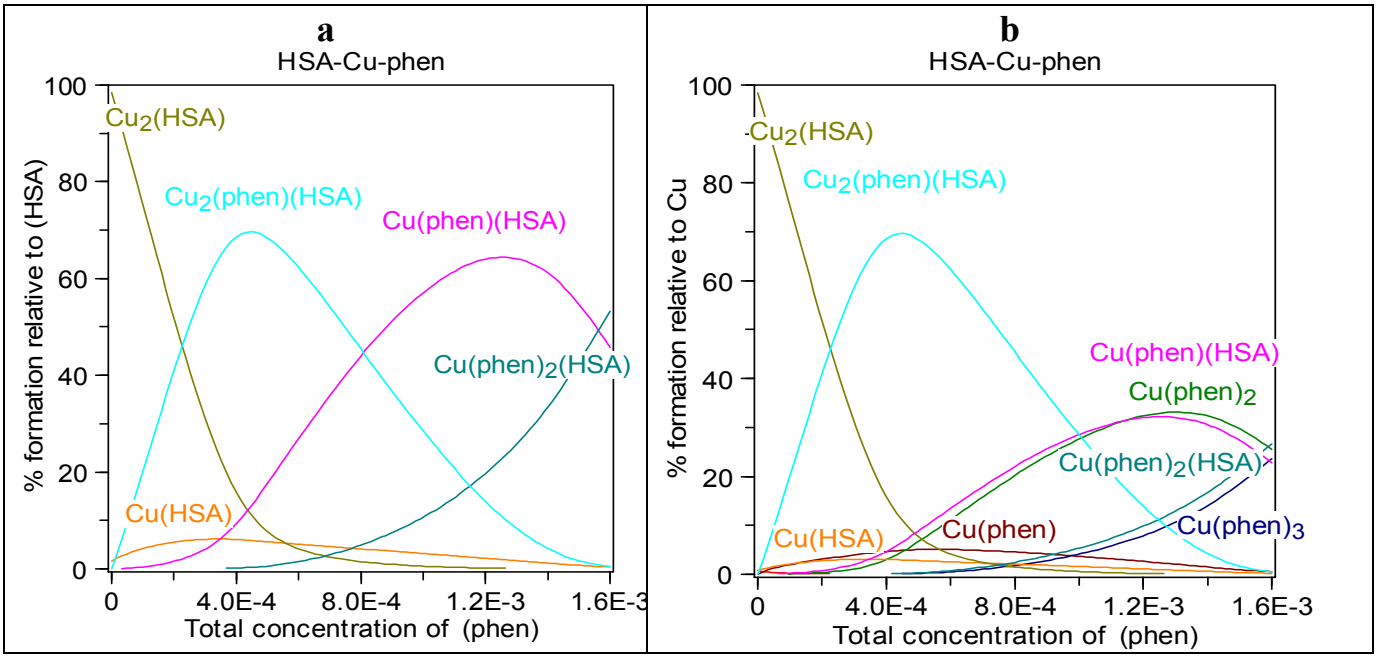

Fig. S15 Species distribution diagrams for the system HSA/Cu = 1:2 with increasing concentrations of phen in solution calculated taking C_{HSA} = 400 μM. (a) speciation for HSA-containing species and (b) speciation for Cu-containing species.

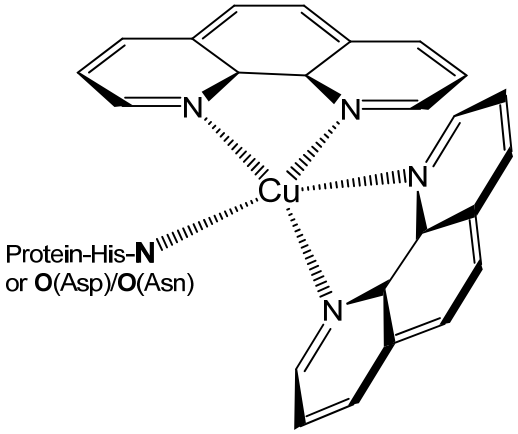

Scheme S1 Probable binding of the Cu^{II} originally bound at site II of HSA in solutions of molar ratios HSA:Cu^{II}:phen of 1:2:2. It is plausible that the binding still involves residues of site II, but the binding set of Cu^{II} changes after addition of phen. Two donor atoms of HSA may be bound to Cu instead of just one as the scheme indicates.

Calculation of Formation constants using the PSEQUAD program

The program PSEQUAD[30] was used to calculate the binding constants for the system HSA-Cu-phen using the CD spectra recorded. To obtain the $\log\beta_{111}$, $\log\beta_{112}$ and molar absorptivities $\Delta\varepsilon_{111}$ and $\Delta\varepsilon_{112}$ for HSA-Cu-(phen) and HSA-Cu-$(phen)_2$, experimental CD spectra of solutions with 200 μM HSA, 200 μM $CuCl_2$ and stepwise additions of phen were used. The logβ values for the OH^-/Cu system, for the HSA/Cu^{II} system and for the Cu^{II}/phen system[23d] were included in the input file of PSEQUAD as fixed: $\log\beta_{110}$(HSA-Cu) = 16.0; $\log\beta_{011}$(Cu(phen)) = 9.10; $\log\beta_{012}$(Cu$(phen)_2$) = 15.85; $\log\beta_{013}$(Cu$(phen)_3$) = 20.9. The log values of binding constants refined were: $\log\beta_{111}$(HSA-Cu-(phen)) = 23.1 ± 0.3 and $\log\beta_{112}$(HSA-Cu-$(phen)_2$) = 28.3 ± 0.4; the calculated $\Delta\varepsilon_{111}$ and $\Delta\varepsilon_{112}$ values obtained by PSEQUAD are compared with the experimental data in Fig. S7 of ESI. Using the program HySS[77] the corresponding species distribution graph may be obtained. It can be observed that at in solutions with e.g. a 1:1:1 HSA:Cu^{II}:phen molar ratio with C_{HSA}= 200 μM, ~82% of the Cu^{II} initially bound at site I is now bound as HSA-Cu-phen, ~8 % as HSA-Cu$(phen)_2$, ~9% as HSA-Cu and ~1% as Cu$(phen)_2$.

The $\log\beta_{111}$, $\Delta\varepsilon_{111}$, $\log\beta_{112}$ and $\Delta\varepsilon_{112}$ obtained were then used in a second input file to obtain the $\log\beta_{121}$, $\Delta\varepsilon_{121}$, $\log\beta_{122}$ and $\Delta\varepsilon_{122}$ values which correspond to HSA-Cu_2-(phen) and HSA-Cu_2-$(phen)_2$ binding. Again, the known logβ values of the relevant species for this system were used as fixed. The log values of the binding constants refined are: $\log\beta_{121}$(HSA-Cu_2-(phen)) = 30.6±0.1 and $\log\beta_{122}$(HSA-Cu_2-$(phen)_2$) = 36.6±0.2 (the SDs presented correspond to the output of PSEQUAD). The calculated $\Delta\varepsilon_{111}$ and $\Delta\varepsilon_{112}$ values obtained by PSEQUAD are compared with the experimental data in Fig. S12 of ESI, the $\Delta\varepsilon_{121}$ and $\Delta\varepsilon_{122}$ values in Fig. S14 of ESI, while all the calculated $\Delta\varepsilon_{111}$, $\Delta\varepsilon_{112}$, $\Delta\varepsilon_{121}$ and $\Delta\varepsilon_{122}$ values are plotted in Figs. S13 of ESI.

Using the program HySS the species distribution graph may be obtained for any particular experimental conditions chosen. Fig S15 of ESI depicts the speciation diagram for HSA:Cu = 1:2 molar ratio, with C_{HSA} = 400 μM and increasing concentrations of phen. For example, with C_{HSA} = 400 μM, C_{Cu} = 800 μM and C_{phen} = 800 μM, ca. ~46% of HSA is present as HSA-Cu_2-(phen), ~42% as HSA-Cu-(phen), ~4% as HSA-Cu_2, 2% as HSA-Cu and ~6% as HSA-Cu_2-$(phen)_2$. In the same conditions, the speciation of Cu^{II} is: ~46% of Cu^{II} is present as HSA-Cu_2-(phen), ~22% as HSA-Cu-(phen), ~3% as HSA-Cu-$(phen)_2$, ~2% as HSA-Cu, ~1% as HSA-Cu_2, ~20% as Cu$(phen)_2$, ~4% as Cu(phen) and ~2% as Cu$(phen)_3$.